Title: Selection bias is unlikely to fully explain the protective effect of childhood adiposity on breast cancer risk.

Article type: Short report.

Authors: Grace M. Power[1,2,3], Eleanor Sanderson[1,2], George Davey Smith[1,2,4]*, Gibran Hemani[1,2]*

*Joint last authors

Affiliations:

1. MRC Integrative Epidemiology Unit, University of Bristol, Bristol, UK.
2. Population Health Sciences, Bristol Medical School, University of Bristol, UK.
3. Institute for Molecular Bioscience, The University of Queensland, Brisbane, Queensland, Australia.
4. NIHR Bristol Biomedical Research Centre Bristol, University Hospitals Bristol and Weston NHS Foundation Trust, University of Bristol, Bristol, UK.

Abstract.

Higher childhood adiposity has been reported to lower breast cancer risk across multiple lines of evidence, including lifecourse Mendelian randomization (MR). These MR results show that the apparent univariable effect of higher adulthood adiposity on lower risk of breast cancer is almost entirely accounted for by the childhood adiposity effect when using multivariable analysis. It has been suggested, however, that this protective effect may arise from collider stratification bias, particularly in selective cohorts such as the UK Biobank.

To examine the plausibility of this claim we first simulated data assuming no true causal effect of adiposity on breast cancer risk to test whether selection bias alone could generate multivariable MR results of the same magnitude as those obtained empirically. Selection into the analytic sample was modelled with log-additive effects of childhood body size and breast cancer status, together with their interaction. Log-additive selection on body size or cancer status alone produced minimal bias. In contrast, interaction-dependent selection generated appreciable downward bias, with the strongest three-way scenario producing the largest spurious protective effect. However, even under these severe scenarios, the bias fell short of the effect observed in earlier MR analyses. Second, we examined if selection bias could induce the joint patterns of univariable and multivariable results observed. We found that across 135k possible models, none strongly overlapped with the observed results, and only 0.7% overlapped with an agreement probability >10%, which mostly relied on a large three-way interaction term between cancer, adulthood body size and childhood body size influencing selection.

To conclude, while selection bias, particularly that which is interaction-driven, can generate spurious protective effects, it is unlikely to fully explain the protective effect of childhood adiposity on breast cancer identified in MR studies.

Introduction.

Experiencing higher adiposity in early life has consistently been associated with a reduced risk of breast cancer across multiple lines of evidence [1-12]. To evaluate the causal nature of this relationship, studies have applied Mendelian randomization (MR), an approach often implemented through using germline genetic variants as instrumental variables [13]. MR analyses have shown that larger prepubertal body size is protective against breast cancer [1-4]. Because alleles are randomly allocated at conception, MR is less susceptible to confounding and reverse causation than conventional epidemiological approaches, strengthening the case for a causal interpretation of this association.

Building on this, lifecourse MR, which employs a multivariable MR framework, uses genetic instruments associated with traits at different developmental periods or ages to estimate direct effects on outcomes, by accounting for the same trait at other life stages [14, 15]. Analyses using this approach show that the direct protective effect of childhood body size on breast cancer remains after accounting for later life adult body size [1–4]. Complementary evidence is provided by a proxy-genotype MR approach, where offspring genotype proxies parental genotype to assess associations with parental disease risk [12].

Whilst MR helps to mitigate confounding, it has been proposed that the observed inverse association may instead reflect selection bias [16, 17], specifically collider stratification bias, which arises from conditioning on a variable influenced by both the exposure and the outcome [18]. This concern is particularly relevant in settings such as the UK Biobank, where participation is selective (5.5% response rate) and recruitment occurs in mid-to-late adulthood [19]. In such designs, both survival to recruitment and voluntary participation may act as colliders if they are affected by childhood adiposity or by breast cancer risk (or their unmeasured common causes). Conditioning in this context may induce noncausal associations, even in the absence of a true causal effect [16]. The extent of this bias is uncertain: while some argue it may be small in practice, its magnitude depends on the underlying causal structure [20]. Banack et al. suggest collider stratification bias exists on a continuum, shaped not only by the strength of causal relations but also by interactions and the prevalence of the collider and its causes [20]. Gkatzionis et al. further show that under log-additive models, with consequences extending to other models of selection, including logistic, bias is driven by interaction terms and may be underestimated if these are ignored [21].

To evaluate whether a protective effect of the magnitude observed could plausibly arise from collider stratification bias, we conducted a series of simulations. Specifically, we aimed to assess whether the direct protective effect of increased childhood body size on breast cancer risk, reported by Richardson et al. using a lifecourse MR approach (OR = 0.59, 95% CI: 0.50 to 0.71; logOR =-0.53, 95% CI:-0.69 to-0.34), could be reproduced through bias alone. By simulating data under the assumption of no true causal effect, we examined whether selection mechanisms could generate an apparent protective effect of similar magnitude. Following this, we also examined the possibility that selection bias could explain the broader pattern of univariable, and multivariable empirical results obtained for body size on breast cancer [1]. In univariable models, both adult and child body size showed modest protective effects on breast cancer. However, in the multivariable model, the protective effect of childhood body size strengthened, while the effect of adulthood body size attenuated to the null. In order to invoke

selection bias as a mechanism to explain the MR results, the selection bias must be able to explain the broader pattern of both univariable and multivariable MR estimates. This allowed us to isolate and quantify the extent to which collider stratification bias might account for the MR findings.

Methods

Latent continuous traits for childhood and adulthood body size were generated from genetic risk scores (GRS). Each GRS was simulated as a standard normal variable (mean zero, standard deviation one), with a genetic correlation of rg=0.67 between childhood and adulthood scores. Each GRS was specified to explain 10% of the variance in its respective body size trait. To capture the empirical observation that body size often persists across the lifecourse, adulthood body size was modelled to depend partly on childhood body size. Specifically, the latent adult body size included a direct contribution from the latent childhood body size (tracking parameter ϕ=0.35), in addition to its own GRS and independent residual noise. This "tracking path" represents the propensity for children who are heavier than their peers to remain heavier in adulthood. All residuals were generated independently, and no further non-genetic correlation was introduced between childhood and adulthood body size.

The latent traits were then discretised into ordinal categories (0 = thinner, 1 = average, 2 = plumper) using thresholds corresponding to the 33rd and 84th percentiles of the UK Biobank distribution. Breast cancer status was assigned randomly using a fixed population prevalence of 1 in 7. We did not introduce confounding between body size and breast cancer risk, as our aim was to examine the influence of selection mechanisms rather than confounding bias.

Simulations used a sample size of n=246,511, chosen to reflect the number of female UK Biobank participants with available relevant data, and were repeated over 500 iterations. Within the selected sample, we estimated the direct effect of childhood body size on breast cancer risk, accounting for adulthood body size, using a two-stage residual inclusion (2SRI) logistic regression model. Breast cancer risk was modelled as a function of both childhood and adulthood body size. In these simulations, breast cancer status was generated independently of body size, so the true causal effect of childhood and adult body size on breast cancer risk was set to zero; any estimated association therefore reflects bias introduced by selection rather than genuine causality. This two-exposure framework mirrors lifecourse MR designs, which jointly instrument early- and later-life body size to estimate the direct effect of childhood adiposity on disease risk, independent of adult adiposity [1]. From each model, we extracted the coefficient for childhood and adult body size to quantify the magnitude and direction of bias introduced under each selection scenario.

The selection mechanisms examined are illustrated in Figure X: Panel A shows the log-additive selection model, and Panel B shows the log-additive + interaction selection model.

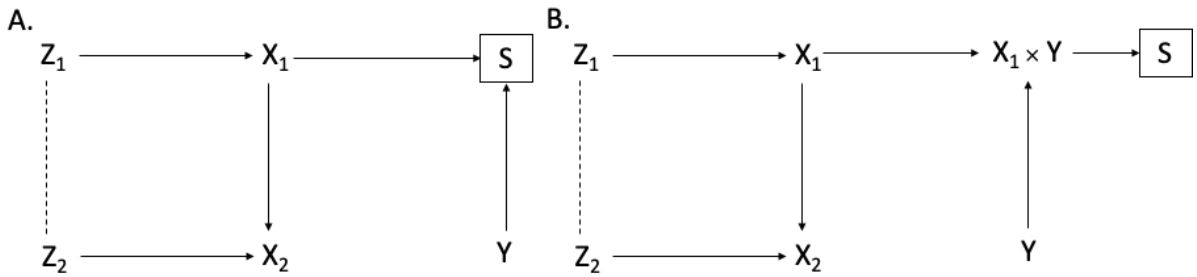

Figure 1. Schematic of the selection mechanism in simulations.

A. Log-additive selection model: childhood (Z_1) and adulthood (Z_2) genetic risk scores (GRS) influence latent childhood (X_1) and adulthood (X_2) body size, respectively, with a genetic correlation (dotted line) between Z_1 and Z_2. Childhood body size (X_1) and breast cancer status (Y) both affect selection into the analytic sample (S). **B.** Log-additive + interaction selection model: in addition to the log-additive effects of X_1 and Y, their joint effect ($X_1 \times Y$) also influences selection (S), reflecting selection probabilities being dependent on both the independent and joint effects of X_1 and Y.

Selection into the analytic sample was modelled using a logistic function with no intercept (Eq. 1).

Eq. 1

$$\text{logit}(P(\text{selected})) = \beta_1 X_1 + \beta_2 X_2 + \beta_3 Y + \beta_4 (X_1 \times Y)$$

where:

- X_1: childhood body size
- X_2: adulthood body size
- Y: binary breast cancer status
- β_1: additive effect of childhood body size on the probability of being selected
- β_2: additive effect of adult body size (fixed at zero)
- β_3: additive effect of breast cancer status on selection
- β_4: interaction effect between childhood body size and breast cancer status, representing differential selection probabilities according to joint values of exposure and outcome

This function defined the data-generating process for selection probability in all simulations. Parameters β_1, β_3, and β_4 directly determined the likelihood of inclusion, rather than assuming a constant participation rate. Negative β_1 values represented preferential inclusion of thinner children; negative β_3 values modelled under-representation of cancer cases; and negative β_4 values represented compounded exclusion of individuals who were both heavier in childhood and developed breast cancer (Table 1).

Table 1. Interpretation of selection parameters.

Mechanism	Parameter	Level	Selection-odds multiplier	Interpretation
Body-size selection	β_1	0.00	1.00	No body-size selection; participants of all childhood body sizes included equally.
		−0.25	0.78 per step	Moderate selection favouring thinner participants; each one-category heavier reduces inclusion odds by 22%.
		−0.50	0.61 per step	Strong selection favouring thinner participants; each one-category heavier reduces inclusion odds by 39% (two steps ≈ 0.37×).
Breast-cancer under-selection	β_3	0.00	1.00 (case vs non-case)	No case under-selection; breast-cancer cases and non-cases included equally.
		−0.25	0.78 (case vs non-case)	Moderate under-selection of breast-cancer cases; cases moderately under-represented.
		−0.50	0.61 (case vs non-case)	Strong under-selection of breast-cancer cases; cases heavily under-represented.
Interaction-dependent selection†	β_4	0.00	1.00	No interaction; body-size and case status act independently (no extra modification for cases by size).
		−0.25	0.78 per step (cases only)	Moderate interaction; heavier breast-cancer cases are additionally less likely to be included, beyond β_1 and β_3.
		−0.50	0.61 per step (cases only)	Strong interaction; compounded exclusion of heavier breast-cancer cases and preferential inclusion of thinner cases, beyond main effects.

† The β_4 multiplier applies in addition to β_1 and β_3 and only to breast-cancer cases; e.g., at $\beta_1 = \beta_3 = \beta_4 = -0.50$, a one-category heavier case has inclusion odds 0.61×0.61×0.61≈0.23 of the reference.

This specification captures two theoretically distinct but potentially co-occurring mechanisms of collider bias (Table 2). Log-additive selection refers to situations where childhood body size and breast cancer status independently affect inclusion in the analytical sample. In contrast, interaction-based selection reflects differential inclusion odds according to joint values of exposure and outcome, such that exclusion is amplified for individuals who were both heavier in childhood and developed breast cancer.

We evaluated all 27 possible combinations of β_1, β_3, and β_4 across none, moderate, and strong levels of selection, spanning settings with no selection bias, log-additive-only bias, and interaction-driven bias.

Table 2. Conceptual mechanisms of selection bias modelled in simulations.

Mechanism	Description	Example contexts
Log-additive selection	Childhood body size and breast cancer status independently affect inclusion in the analytical sample.	Heavier children lost to follow-up due to long-term health conditions or socioeconomic disadvantage; breast cancer cases underrepresented due to earlier mortality or lower participation.
Interaction-based selection	Inclusion depends jointly on childhood body size and breast cancer status, such that exclusion is amplified for heavier individuals who also develop breast cancer.	Heavier children who later develop breast cancer less likely to be recruited due to compounded health risks, earlier death, or structural disadvantage.

We next extended the biasing model to explore if selection could explain the broader pattern of univariable and multivariable results observed empirically (Eq. 2).

Eq. 2

$$\text{logit}(P(\text{selected})) = \beta_1 X_1 + \beta_2 X_2 + \beta_3 Y + \beta_4(X_1 \times Y) + \beta_5(X_2 \times Y) + \beta_6(X_1 \times X_2 \times Y)$$

where:

- β_5: interaction effect between adulthood body size and breast cancer status, representing differential selection probabilities according to joint values of exposure and outcome
- β_6: interaction effect between childhood body size, adulthood body size and breast cancer status, representing differential selection probabilities according to joint values of exposure and outcome.

For these simulations we allowed all selection coefficients to vary across the range (0, -0.1, …, -0.6). We obtained four estimates – the univariable and multivariable effects of body size on cancer for childhood and adulthood each. To examine if the selection mechanism of a particular simulation could explain the empirical result we calculated the $p(overlap) = \prod_i^4 p_i$

where $z_i = abs(\hat{\beta}_{sim} - \hat{\beta}_{empirical}) / \sqrt{\sigma_{sim}^2 + \sigma_{empirical}^2}$ and p_i is the two-tailed probability of z_i being drawn from a standard normal distribution. The empirical results published in Richardson et al. [1] are provided in Table 3.

Table 3. Empirical results for the effect of body size on breast cancer risk from Richardson et al 2020.

Timepoint	Method	OR (95% CI)
Adulthood	Univariable	0.82 (0.73, 0.92)
Childhood	Univariable	0.63 (0.55, 0.72)
Adulthood	Multivariable	1.08 (0.93, 1.27)
Childhood	Multivariable	0.59 (0.50, 0.71)

Results.

Our simulations indicate that selection bias alone is unlikely to explain the protective MR estimate for childhood adiposity on breast cancer (empirical logOR = -0.53); only under implausibly strong interaction-driven selection scenarios did simulated estimates move towards this value. We evaluated 27 scenarios varying three selection mechanisms – body-size selection (more negative values preferentially include thinner individuals), breast-cancer selection (more negative values preferentially exclude cases), and an interaction between body size and case status (more negative values preferentially include thinner participants without breast cancer and exclude heavier cases) – each at three prespecified intensities (none, moderate, strong), with 500 replicates per scenario. Intensity levels correspond to per-step inclusion odds ratios of 1.00 (none), 0.78 (moderate), and 0.61 (strong) (Table 1).

With no interaction, mean logORs ranged from -0.06 to 0.01 across all combinations of body-size and cancer selection, and the empirical MR value was never contained by replicate-level 95% confidence intervals (coverage 0% in all nine scenarios; Table 4; Figure 2-3). With moderate interaction, mean logORs ranged from -0.21 to -0.12 and coverage was 0–5%, with non-zero coverage only when both traits were under selection. With strong interaction, mean logORs ranged from -0.36 to -0.23 and coverage was 2-48%, increasing with the strength of selection on both traits; the most negative average occurred under the strongest three-way combination (body size strong, cancer selection strong, interaction strong), yielding a mean logOR of -0.36 (SD 0.09; mean SE 0.09; coverage 48%). Scenarios with selection on only one trait produced estimates close to zero (body size only: -0.01; cancer only: 0.00; both 0% coverage). Interaction-only selection produced mean logORs of -0.13 (moderate interaction; 0% coverage) and -0.25 (strong interaction; 2% coverage). The R^2 patterns presented in Table 4 highlight that only when the interaction explained a substantial fraction of the selection variance did estimates begin to move toward the empirical value.

Across all scenarios, adult effect estimates were centred on zero, with mean logORs ranging from -0.01 to 0.01 (SD 0.06-0.07), showing that the simulated selection mechanisms did not induce bias in adulthood effect estimates.

Taken together, these results (Table 4; Figures 2-3) indicate that interaction-dependent selection induces progressive downward bias as selection pressures increase, yet even under the strongest setting the mean logOR (-0.36) remained less negative than the empirical MR estimate (-0.53).

Table 4. Simulation results across 27 parameter scenarios of log-additive and interaction-based selection.

For each scenario, we report the mean estimated log odds ratio (logOR) for childhood body size, its standard deviation (SD), and the mean standard error (SE) across 500 replicates. Equivalent columns are also reported for adult body size estimates. The R^2 columns show the proportion of variance in the selection liability explained by childhood body size (β_1), breast cancer status (β_3), and their interaction (β_4). Percentages may not sum to 100% because a residual overlap (cross-term) between the childhood and interaction components is omitted. In the "no selection" setting ($\beta_1 = \beta_3 = \beta_4 = 0$), the variance of the selection liability is zero and component shares are undefined.

β1 - child body size selection	R^2 of selection - child body size %	β3 - breast cancer selection	R^2 of selection - breast cancer %	β4 - interaction selection	R^2 of selection - interaction %	Mean logOR (Child)	SD logOR (Child)	Mean SE (Child)	Mean logOR (Adult)	SD logOR (Adult)	Mean SE (Adult)
-0.50	66%	-0.50	14%	-0.50	19%	-0.356	0.085	0.085	-0.001	0.065	0.066
-0.50	72%	-0.50	17%	-0.25	11%	-0.210	0.086	0.085	-0.003	0.072	0.066
-0.50	74%	-0.50	21%	0.00	5%	-0.061	0.084	0.085	0.001	0.063	0.066
-0.50	74%	-0.25	4%	-0.50	22%	-0.305	0.081	0.080	0.005	0.061	0.062
-0.50	82%	-0.25	6%	-0.25	13%	-0.168	0.075	0.080	0.002	0.060	0.062
-0.50	88%	-0.25	6%	0.00	7%	-0.027	0.079	0.080	-0.004	0.061	0.062
-0.50	77%	0.00	0%	-0.50	23%	-0.234	0.078	0.076	-0.006	0.060	0.059
-0.50	85%	0.00	0%	-0.25	15%	-0.123	0.073	0.076	0.001	0.059	0.059
-0.50	93%	0.00	0%	0.00	7%	-0.005	0.072	0.075	0.004	0.057	0.059
-0.25	43%	-0.50	32%	-0.50	25%	-0.340	0.085	0.082	0.004	0.068	0.066
-0.25	47%	-0.50	38%	-0.25	15%	-0.192	0.083	0.082	0.003	0.066	0.066
-0.25	43%	-0.50	54%	0.00	4%	-0.029	0.084	0.082	0.001	0.067	0.066
-0.25	54%	-0.25	10%	-0.50	36%	-0.293	0.079	0.078	0.002	0.062	0.062
-0.25	64%	-0.25	17%	-0.25	20%	-0.149	0.082	0.077	-0.003	0.063	0.062
-0.25	74%	-0.25	20%	0.00	6%	-0.020	0.079	0.077	0.003	0.064	0.062
-0.25	60%	0.00	0%	-0.50	40%	-0.249	0.072	0.073	-0.002	0.059	0.059
-0.25	78%	0.00	0%	-0.25	22%	-0.129	0.072	0.073	0.001	0.060	0.059
-0.25	94%	0.00	0%	0.00	6%	0.006	0.073	0.073	-0.003	0.060	0.059
0.00	3%	-0.50	66%	-0.50	31%	-0.313	0.080	0.081	0.003	0.064	0.066
0.00	1%	-0.50	89%	-0.25	11%	-0.163	0.081	0.081	0.002	0.067	0.066
0.00	0%	-0.50	100%	0.00	0%	0.002	0.080	0.081	-0.004	0.063	0.066
0.00	5%	-0.25	32%	-0.50	63%	-0.281	0.074	0.076	0.002	0.062	0.062
0.00	4%	-0.25	63%	-0.25	33%	-0.140	0.077	0.076	0.002	0.064	0.062
0.00	0%	-0.25	100%	0.00	0%	0.002	0.076	0.075	-0.001	0.059	0.062
0.00	9%	0.00	0%	-0.50	91%	-0.247	0.068	0.072	-0.002	0.058	0.059
0.00	6%	0.00	0%	-0.25	94%	-0.126	0.075	0.072	0.002	0.059	0.059
0.00	NA	0.00	NA	0.00	NA	0.003	0.073	0.071	-0.005	0.058	0.059

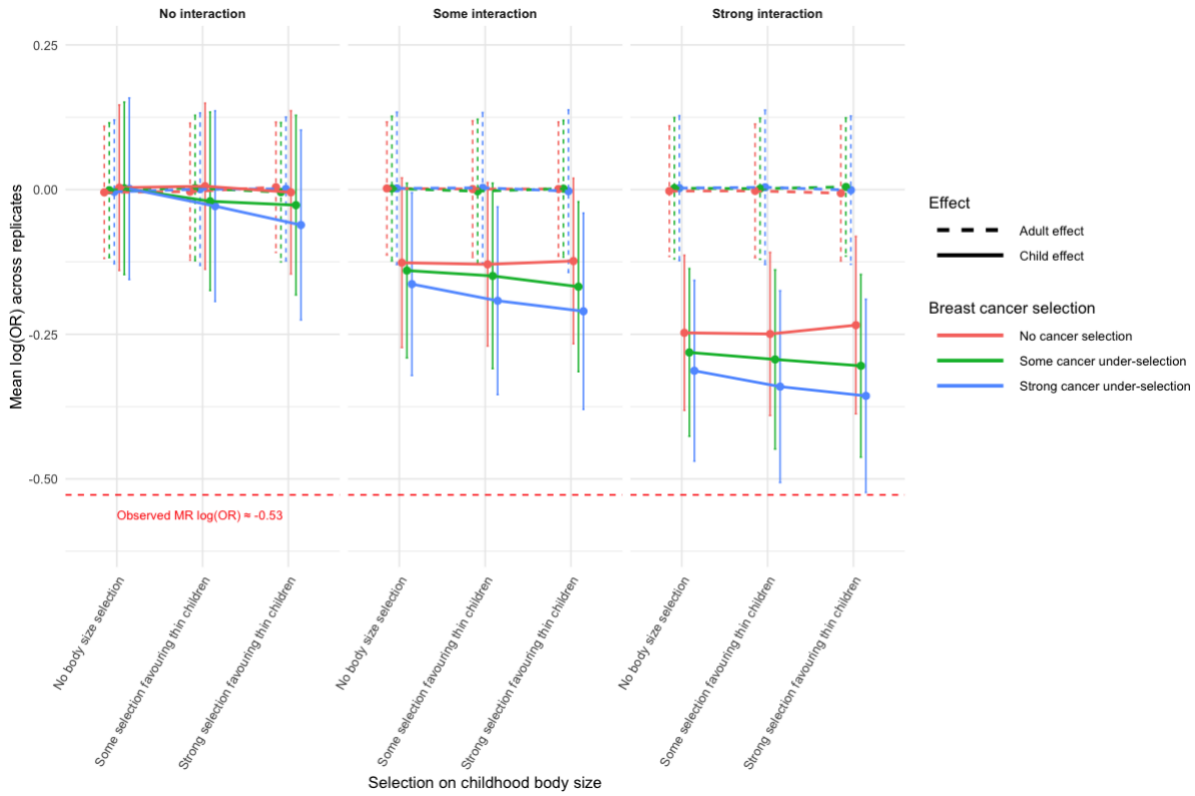

Figure 2. Simulated bias under varying selection scenarios. Mean log(OR) estimates for childhood (solid) and adult (dashed) body size on breast cancer across 500 replicates are shown under increasing strengths of body-size and breast-cancer selection, with panels representing different levels of interaction. Error bars indicate the 2.5th–97.5th percentile range. The red dashed line marks the observed childhood MR estimate (logOR = –0.53).

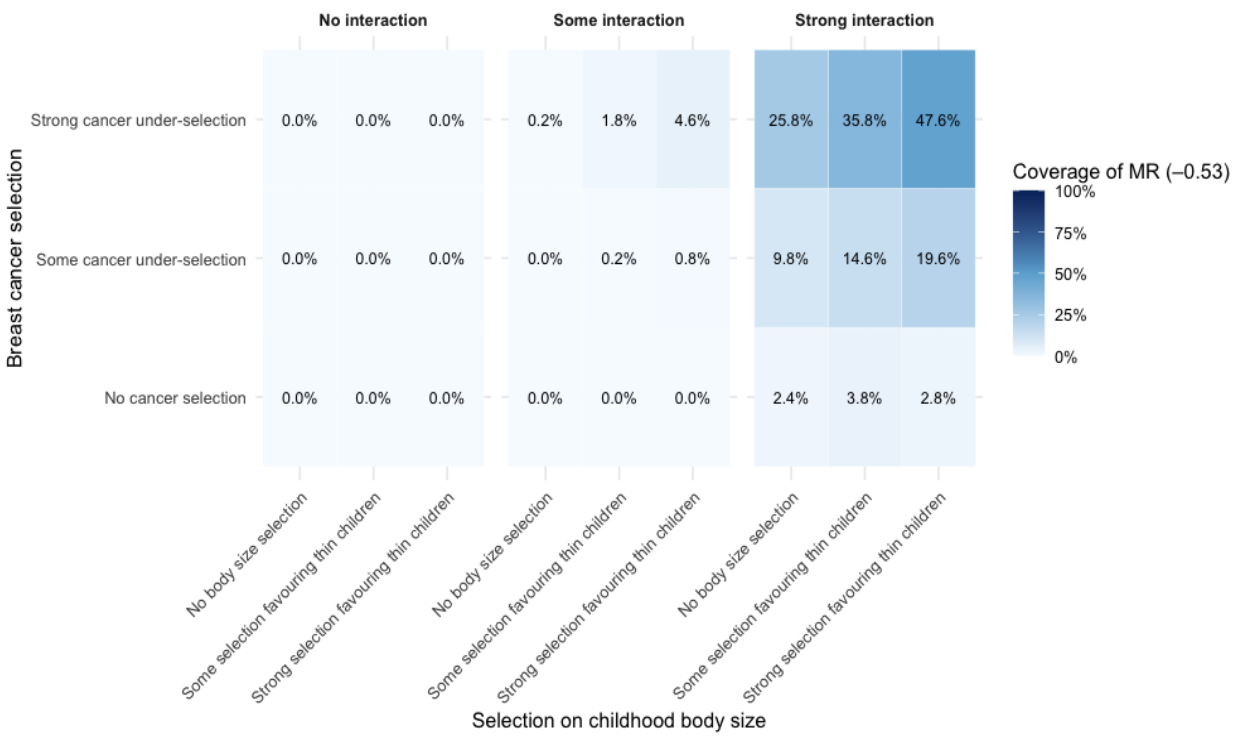

Figure 3. Coverage of the empirical MR estimate across selection scenarios.
Heatmap displaying the proportion of simulation replicates in which the empirical MR estimate (logOR =-0.53) was contained within the 95% confidence interval. Columns represent levels of interaction-dependent selection, rows represent levels of breast cancer selection, and the x-axis shows childhood body size selection. Cell shading reflects coverage percentage, from 0% (white) to 100% (dark blue).

We next examined if selection bias could be used to induce the broader pattern of univariable and multivariable effect estimates shown in Table 3. Across the range of approximately 135,000 simulation scenarios, 2.5% resulted in all four simulation estimates being 'consistent' with empirical estimates (Figure 4). This is using a relaxed definition of 'consistent' where the probability of overlap exceeded 5%. However, only 0.19% of models had a joint probability of overlap across all four models exceeding 5%. To induce such effects, specific patterns of selection bias were required including a three-way interaction term where cancer, childhood body size and adulthood body size all interacted to influence selection (Figure 5).

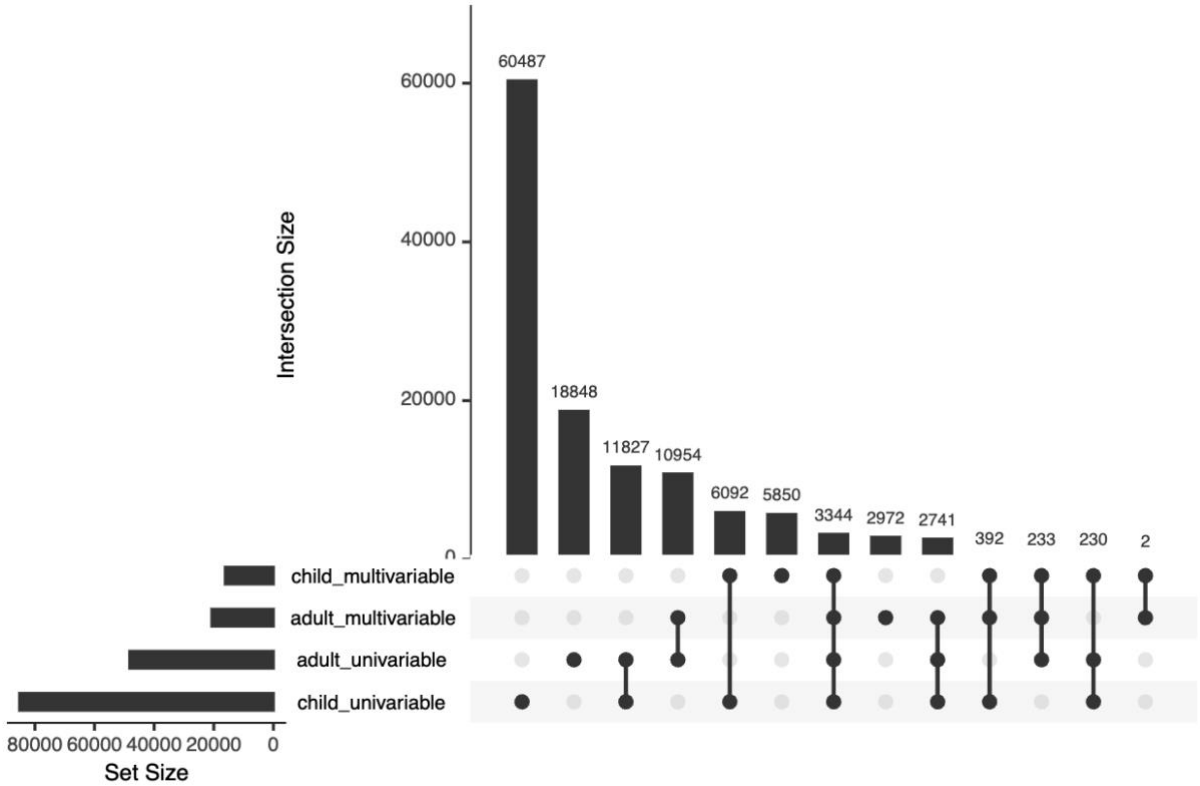

Figure 4: UpSet plot showing the simulation models that agreed with empirical results with per-estimate overlap probability > 10%.

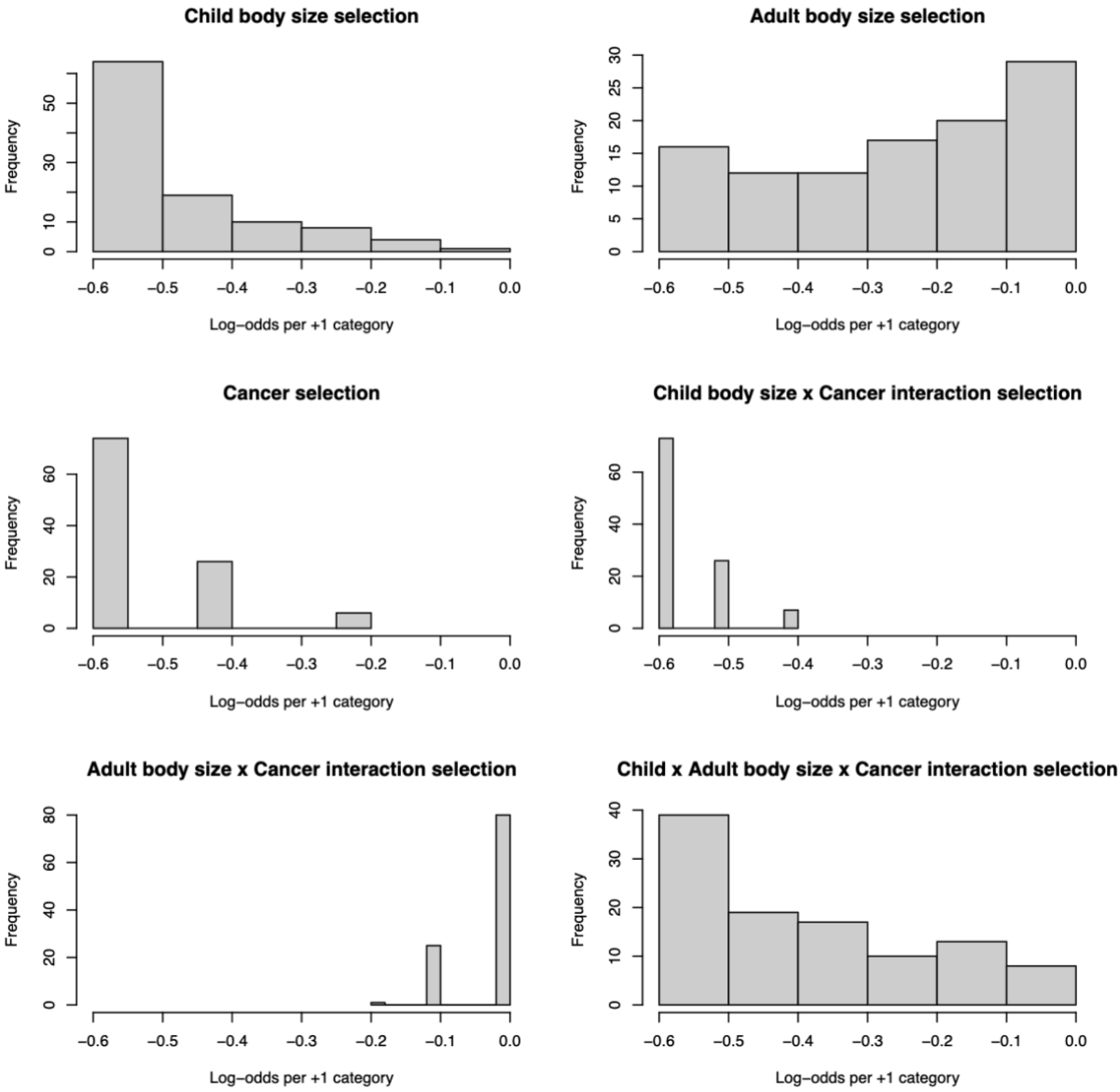

Figure 5: Distribution of selection parameters required to induce selection bias in simulations that led to estimates that agreed with the empirical models with joint overlap probability > 10%.

Discussion.

In this study, we set out to examine whether the protective effect of increased childhood body size on breast cancer risk, derived through previous lifecourse Mendelian randomization (MR) analyses (logOR = -0.53) [1], could be reproduced by collider stratification bias alone. We simulated data under the assumption of no true causal effect and applied a lifecourse MR analytic framework to assess whether selection mechanisms could generate an effect of the magnitude observed. As has been suggested [16, 17], the observed inverse association may partly be an artifact of survival-related selection. Our simulations directly address this possibility.

Our findings demonstrate that while selection bias can induce spurious protective effects, the strongest biases observed in our simulations (mean logOR =-0.36) fell short of the empirical MR estimate. Importantly, achieving this level of bias required severe and simultaneous selection pressures on childhood body size, breast cancer status, and their interaction.

When log-additive selection acted in isolation, the corresponding variable explained the majority of the variance in selection (up to 93% for childhood body size and 100% for breast cancer status), but even this produced only negligible collider bias. Under strong interaction-dependent selection alone, the interaction term explained 91% of the variance in selection and was sufficient to generate bias. When strong log-additive and interaction pressures operated together, the variance in selection was shared across body size (66%), cancer status (14%), and their interaction (19%). This joint scenario produced the strongest biased estimate in our simulations (logOR = -0.36), with the interaction component driving the effect. In our simulations, adulthood estimates remained close to zero across all scenarios, as expected given that no causal effects were specified and selection acted only on childhood body size and breast cancer status. This reassures that the simulated bias did not spill over to induce artefactual associations at other ages.

We additionally examined whether selection bias could reproduce the broader pattern of univariable and multivariable estimates reported empirically. While some simulations produced estimates individually consistent with the empirical effects, fewer than 0.2% of scenarios were able to reproduce all four jointly within a single run. Achieving this required highly restrictive and implausible conditions: a strong three-way interaction in which childhood body size, adulthood body size, and breast cancer status jointly influenced selection, and simultaneously no interaction between adulthood body size and breast cancer. Together, these conditions were necessary to induce the empirical pattern, where both childhood and adulthood body size appeared protective in univariable models, but only childhood body size remained protective in multivariable models.

These findings underscore several key insights. First, explaining a large share of selection variance does not necessarily imply bias; log-additive selection can dominate inclusion without distorting exposure-outcome associations. Second, collider bias only became appreciable when the interaction term captured a substantial share of variance, reflecting compounded exclusion of individuals who were both heavier in childhood and developed breast cancer. Even then, the induced bias was insufficient to fully reproduce the MR estimate. Third, reproducing the

empirical profile of previously derived MR effects occurred only under very rare and restrictive selection structures, specifically strong three-way interactions.

These results align with theoretical work emphasising the critical role of interaction-dependent selection in driving collider bias [20, 21]. They also provide empirical reassurance that although selective participation and survival occur in UK Biobank, the degree of interaction-driven exclusion required to generate the observed MR estimate appears implausibly strong. Bias may therefore contribute partially but cannot fully explain the robust protective association consistently observed across MR studies.

There is often a question over whether MR results might be explained by selection bias, which can be very difficult to measure. Simulations such as these may be an effective way to examine the risk of such biases driving observed associations. Another key strength of our study is the use of large-scale simulations closely mirroring the lifecourse MR framework, allowing us to directly test whether collider stratification bias could reproduce the observed protective effect. We also quantified how much variance in selection was attributable to body size, cancer status, and their interaction, and offered novel insights into the mechanisms underpinning selection bias. However, our simulation approach also has limitations. First, real-world selection is likely more complex than the mechanisms we modelled, potentially involving correlated health traits and socio-demographic factors. Next, while our prevalence parameters reflected real-world breast cancer risk, they may not fully capture participation dynamics in UK Biobank, where recruitment and survival processes may differ from the general population.

Conclusion.

While selection bias can influence MR estimates, our findings suggest that the strong protective effect of higher childhood adiposity on breast cancer is unlikely to be fully explained by such mechanisms. Only interaction-based selection generated appreciable bias, and even under extreme conditions estimates did not reach the magnitude observed empirically. Moreover, reproducing the full pattern of univariable and multivariable MR estimates observed previously was only possible under rare and restrictive scenarios, underscoring the implausibility of selection bias as a sole explanation.

References.

1. Richardson, T.G., et al., *Use of genetic variation to separate the effects of early and later life adiposity on disease risk: mendelian randomisation study.* BMJ, 2020. **369**: p. m1203.
2. Hao, Y., et al., *Reassessing the causal role of obesity in breast cancer susceptibility: a comprehensive multivariable Mendelian randomization investigating the distribution and timing of exposure.* Int J Epidemiol, 2023. **52**(1): p. 58-70.
3. Power, G.M., et al., *A structural mean modelling Mendelian randomization approach to investigate the lifecourse effect of adiposity: applied and methodological considerations.* American Journal of Epidemiology, 2025.
4. Vabistsevits, M., et al., *Deciphering how early life adiposity influences breast cancer risk using Mendelian randomization.* Commun Biol, 2022. **5**(1): p. 337.
5. Jensen, B.W., et al., *Childhood body mass index trajectories, adult-onset type 2 diabetes, and obesity-related cancers.* J Natl Cancer Inst, 2023. **115**(1): p. 43-51.
6. Fagherazzi, G., et al., *Body shape throughout life and the risk for breast cancer at adulthood in the French E3N cohort.* European Journal of Cancer Prevention, 2013. **22**(1): p. 29-37.
7. Song, M., et al., *Trajectory of body shape across the lifespan and cancer risk.* Int J Cancer, 2016. **138**(10): p. 2383-95.
8. Yang, T.O., et al., *Body size in early life and the risk of postmenopausal breast cancer.* BMC cancer, 2022. **22**(1): p. 232.
9. Llewellyn, A., et al., *Childhood obesity as a predictor of morbidity in adulthood: a systematic review and meta-analysis.* Obesity reviews, 2016. **17**(1): p. 56-67.
10. Byun, D., et al., *Early-life body mass index and risks of breast, endometrial, and ovarian cancers: a dose-response meta-analysis of prospective studies.* Br J Cancer, 2022. **126**(4): p. 664-672.
11. Andersen, Z.J., et al., *Birth weight, childhood body mass index, and height in relation to mammographic density and breast cancer: a register-based cohort study.* Breast Cancer Research, 2014. **16**(1): p. R4.
12. Richardson, T.G., et al., *Leveraging family history data to disentangle time-varying effects on disease risk using lifecourse mendelian randomization.* European Journal of Epidemiology, 2023. **38**(7): p. 765-769.
13. Davey Smith, G., *Mendelian Randomization for Strengthening Causal Inference in Observational Studies:Application to Gene × Environment Interactions.* Perspectives on Psychological Science, 2010. **5**(5): p. 527-545.
14. Sanderson, E., et al., *Estimation of causal effects of a time-varying exposure at multiple time points through multivariable mendelian randomization.* PLoS Genet, 2022. **18**(7): p. e1010290.
15. Power, G.M., et al., *Methodological approaches, challenges, and opportunities in the application of Mendelian randomisation to lifecourse epidemiology: A systematic literature review.* Eur J Epidemiol, 2024. **39**(5): p. 501-520.
16. Schooling, C.M., K. Fei, and J.V. Zhao, *Selection bias as an explanation for the observed protective association of childhood adiposity with breast cancer.* J Clin Epidemiol, 2023. **164**: p. 104-111.

17. Schooling, C.M., K. Fei, and M.B. Terry, *Reassessing the causal role of early-life adiposity in breast cancer: could the apparent inverse associations be a manifestation of survival bias?* International Journal of Epidemiology, 2023. **52**(4): p. 1292-1293.
18. Banack, H.R., et al., *Collider Stratification Bias I: Principles and Structure.* American Journal of Epidemiology, 2023. **193**(2): p. 238-240.
19. Batty, G.D., et al., *Comparison of risk factor associations in UK Biobank against representative, general population based studies with conventional response rates: prospective cohort study and individual participant meta-analysis.* Bmj, 2020. **368**: p. m131.
20. Banack, H.R., et al., *Collider stratification bias II: magnitude of bias.* Am J Epidemiol, 2025. **194**(5): p. 1149-1151.
21. Gkatzionis, A., et al., *Relationship between collider bias and interactions on the log-additive scale.* Stat Methods Med Res, 2025: p. 9622802241306860.

Sources of funding.

GMP, ES, GH, and GDS were supported by the Integrative Epidemiology Unit which receives funding from the UK Medical Research Council and the University of Bristol (MC_UU_00032/1). GMP was additionally supported by the University of Bristol Cancer research fund for this work. GDS conducts research at the NIHR Biomedical Research Centre at the University Hospitals Bristol NHS Foundation Trust and the University of Bristol.

Research Ethics and Informed Consent.

This study was based entirely on simulated data and did not involve human participants directly; therefore, no ethical approval or informed consent was required.

Conflicts of interest.

Authors declare no conflict of interest.

Data and computing code availability.

All code used to generate the simulations and reproduce the results reported here is publicly available at https://github.com/gracemarionpower/selection-bias-simulations/. The data underlying the findings can be derived directly from these simulations.